minerals

Article

Particle Classification in the Enhanced Gravity Field Using the Knelson Concentrator

Ling Zhang [1,2], Lu Yang [1,3,*], Yan Zhao [1], Haochun Hou [1], Zeliang Zhang [1], Jun Lin [1], Caiyun Bu [1], Xinran Zheng [1] and Dong Fu [4]

[1] School of Resources and Environmental Engineering, Shandong University of Technology, Zibo 255000, China; zlpass@sdut.edu.cn (L.Z.)
[2] Xinjiang Engineering Technology Research Center of Biological Solid Waste Recycling, Kashi University, Kashgar 844006, China
[3] Sichuan Sizhong Basalt Fiber Technology Research and Development Co., Ltd., Dazhou 635000, China
[4] School of Chemistry and Chemical Engineering, Sichuan University of Arts and Science, Dazhou 635000, China
* Correspondence: ylpass@sdut.edu.cn

Abstract: The particle classification in the enhanced gravity field generated by the Knelson concentrator was studied in this paper. Three main test parameters, namely rotation speed, backwash water pressure, and solid mass percentage, that affected the classification performance of the Knelson concentrator for the classification tests of quartz and synthetic ore, which consisted of quartz and magnetite, were investigated. The yield of quartz concentrate increased with the rotation speed and decreased with the solid mass percentage and backwash water pressure. A lower backwash water pressure and solid mass percentage could improve the classification efficiency. The classification performance of the Knelson concentrator was comparable to that of the traditional hydrocyclone, with a classification efficiency of 76.84% and cut size of 49 µm when the solid mass percentage was 16.67%, the backwash water pressure was 50 kPa, and the rotation speed was 3600 rpm. The classification performance of quartz in synthetic ore tests was inferior to the single quartz tests, and the magnetite showed a better classification efficiency than the quartz with the same combination of test parameters. This study revealed the classification performance in the separation process of the Knelson concentrator in detail, which was beneficial for clarifying the migration rule of fine-grained minerals in the enhanced gravity field.

Keywords: classification efficiency; particle separation; Knelson concentrator; enhanced gravity field

check for updates

Citation: Zhang, L.; Yang, L.; Zhao, Y.; Hou, H.; Zhang, Z.; Lin, J.; Bu, C.; Zheng, X.; Fu, D. Particle Classification in the Enhanced Gravity Field Using the Knelson Concentrator. *Minerals* **2023**, *13*, 1295. https://doi.org/10.3390/min13101295

Academic Editors: Carlos Hoffmann Sampaio and Chiharu Tokoro

Received: 5 September 2023
Revised: 3 October 2023
Accepted: 4 October 2023
Published: 5 October 2023

1. Introduction

Mineral particle size significantly impacts the unit operation efficiency in traditional mineral engineering techniques, such as flotation, gravity separation, magnetic separation, and electrostatic separation, and, in general, a narrower particle size range is advantageous for improving the operation efficiency. Screening and classification are usually used to divide a wide mineral particle size range into different narrow ones [1,2]. The industrial wet classification equipment can be categorized into three types: hydraulic classifier (Floatex Separator and CrossFlow Separator) [3,4], mechanical classifier (spiral classifiers and rake classifier) [5,6], and centrifugal classifier (hydrocyclone) [7,8]. The centrifugal classifier has become the dominant classification equipment for fine particle sizes, especially for the size range of about −200 µm in closed grinding circuits [9–11]. The classification equipment utilizes the settling speed difference of different mineral particles in the fluid medium to divide the fine particles into two or more narrow size ranges, and the process is not only related to the particle size but also to their specific gravity and shape [12,13].

Broadly speaking, the principles of classification and gravity separation are the same, as particle separation is accomplished based on the differences in the settling velocity of particles; meanwhile classification and separation are concomitant and inseparable [14]. However, classification and gravity separation are separate unit operation processes in mineral processing plants. In the classification process, particle size is the focus of the separation, while in the gravity separation process, minerals are separated mainly based on the density difference. Enhanced gravity separation (EGS) is an effective technique for treating fine-grained minerals (−0.5 mm) with lower capital, low costs, and larger treating capacity [15–17]. The Knelson concentrator (KC), as a representative gravity separator, was developed in 1978 and commercialized in the early 1980s and has now been improved over four generations [18,19]. It was widely used in precious metal recovery, including gold ore, copper ore, tin ore, etc. [20–22].

In most research, KCs were used to concentrate gold ores [23,24], synthetic ore [25,26], coal [27], nonmetallic minerals [28], jewelry wastes [29], etc. Xiao et al. modeled and predicted the gold recovery of a −800 μm gold deposit by using the Gravity Recoverable Gold (GRG) test [30]. Ghaffari et al. investigated the separation performance of the KC for −600 μm synthetic ore (quartz, magnetite, ferromolybdenum, copper, zinc, and lead) [31]. Özgen et al. used the KC to separate coal-washing-plant tailings of −500 μm and achieved a maximum combustible recovery of 81.61% [27]. Chen et al. studied the distribution of a quartz sample with a particle size range of −650 + 550 μm, −380 + 270 μm, −250 + 212 μm, and −180 + 150 μm in different rings in the bowl [32]. Burat et al. used the KC to separate jewelry wastes, which were crushed to −150 μm and recovered up to 92% of Au and Ag [29]. These findings suggested that mineral particle sizes were considered, indicating that mineral particle sizes were crucial to the gravity separation process. However, the classification closely related to mineral particle sizes had received little attention.

Different from traditional studies using the KC to investigate the mineral separation process [29,30], this work focuses on the classification of particles in the enhanced gravity field, that is, the classification performance of the laboratory KC by treating the natural minerals of quartz and synthetic ore composed of magnetite and quartz. The test parameters were the rotation speed, backwash water pressure, and solid mass percentage. The sharpness index, imperfection, and classification efficiency were used to evaluate the classification performance of KC, and its performance with hydrocyclones was also compared. Revealing the classification performance of the KC is beneficial for clarifying the migration rule of fine particles in the enhanced gravity field and optimizing the separation effect and classification effect of the KC from the perspective of particle size.

2. Materials and Methods

2.1. Materials and Classification Apparatus

The classification test rig used in this investigation was the Knelson MD−3. The inverted and multi-hole KC bowl was mounted on a rotating shaft. As shown in Figure 1, there are five rings from the bottom to the top, with increasing diameters inside the bowl, and each ring has a number of 1 mm diameter tangentially oriented holes evenly spaced. The KC depends on an enhanced gravitational force, along with a fluidization process to recover fine particles. First, the backwash water is injected from the oriented holes in each ring. Then, the slurry is introduced into the rotational bowl from a feed pipe. Mineral particles of different densities are fluidized under the effect of backwash water and enhanced gravitational force, and, eventually, the denser particles settle in the ring, and the less dense mineral particles are flushed out to become tailings.

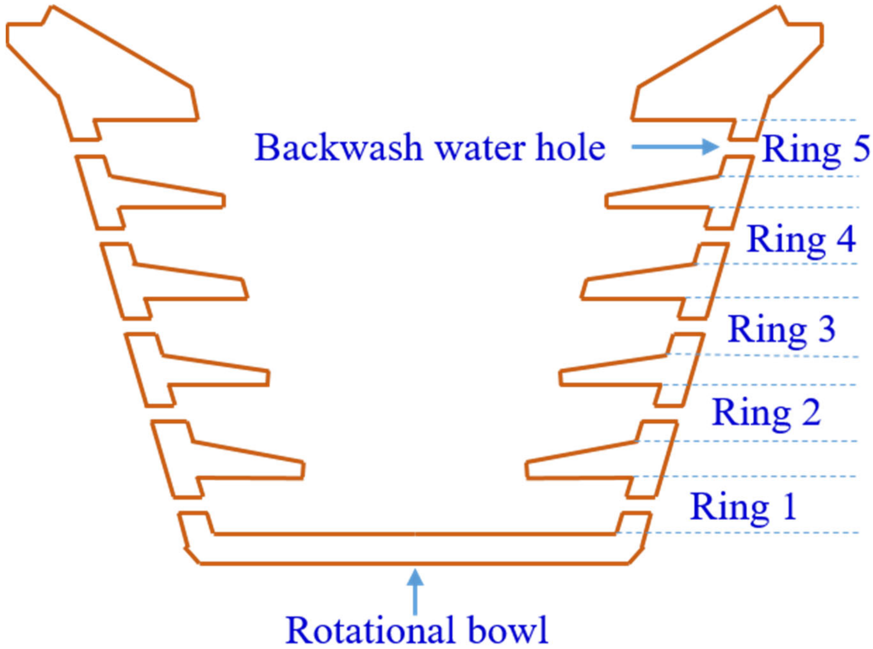

Figure 1. The scheme for the rotational bowl.

Single mineral particles such as quartz and magnetite are often used as raw materials for mineral separation experiments [11,26,27,31]. In this study, quartz powder (Xinyi silica Co., Ltd., Xinyi, China) and synthetic ore consisting of quartz and magnetite powder (Jinling iron ore mine, Zibo, China) with a mass ratio of 1:1 were used to mimic natural minerals with the same densities. The XRD pattern images in Figures 2 and 3 show that the samples used for tests were predominantly quartz and magnetite with high purity. The size distributions of quartz and magnetite are shown in Table 1. The proportion of −500 μm particles in raw quartz was 96.71%, and most particles were concentrated below 400 μm, accounting for 89.98%. The percentage of −200 μm particles in raw magnetite was 92.93%, and it showed that the raw magnetite is finer than the raw quartz.

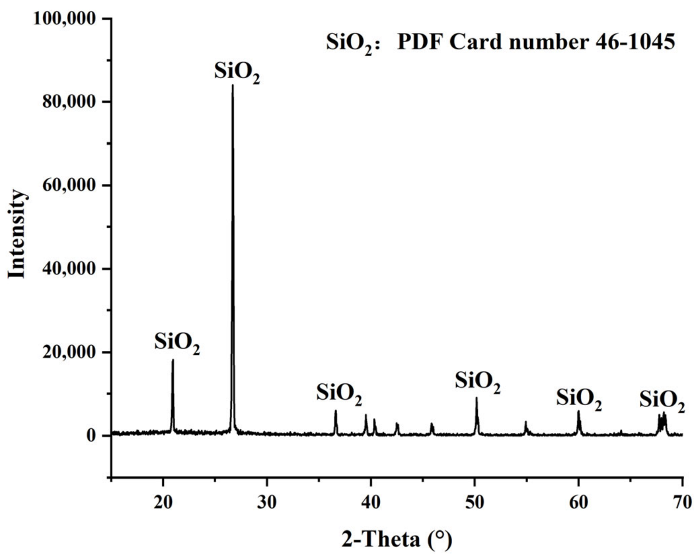

Figure 2. The XRD pattern of quartz.

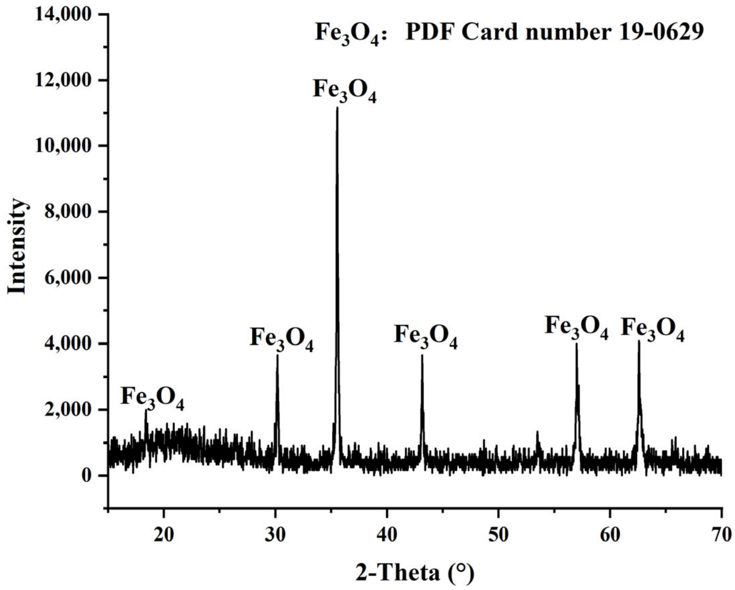

Figure 3. The XRD pattern of magnetite.

Table 1. Size distribution of quartz and magnetite.

Size Range (μm)	Mass Proportion in Size Class (%)			
	Quartz		Magnetite	
	Individual	Cumulative	Individual	Cumulative
−5	0	0	0	0
−10 + 5	0	0	1.03	1.03
−20 + 10	0.20	0.20	4.26	5.29
−45 + 20	2.50	2.7	12.60	17.89
−75 + 45	4.45	7.15	19.62	37.51
−100 + 75	4.05	11.2	17.18	54.69
−200 + 100	32.61	43.81	38.24	92.93
−300 + 200	32.21	76.02	5.88	98.81
−400 + 300	13.96	89.98	1.04	99.85
−500 + 400	6.73	96.71	0.15	100
+500	3.29	100	0	100

2.2. Classification Tests

The tests were conducted to obtain the classification performance with a designed experimental process. Three test parameters, namely solid mass percentage, backwash water pressure, and rotation speed, that significantly affected the classification process were studied, and the range of test parameters is shown in Table 2. The quartz or synthetic ore samples used for classification tests are obtained from sample preparation and sample division with the required division variance. Although there may be slight errors in the composition and particle size of the test samples, the errors can be almost ignored in the classification results in the study.

Table 2. Classification test parameters.

Test Parameters	Value
Solid mass percentage/%	9.09, 16.67, 23.08
Rotation speed/rpm	600, 1200, 1800, 2400, 3000, 3600
Backwash water pressure/kPa	35, 50, 100, 150, 200

For each test, a solid mass of 50 g, 100 g, and 150 g is added to 500 g water to form a solid mass percentage of 9.09%, 16.67%, and 23.08%, respectively. For the single quartz tests, the sample volumes correspond, respectively, to 519 cm^3, 537 cm^3 and 556 cm^3; and for synthetic ore tests, they correspond to 514 cm^3, 523 cm^3, and 533 cm^3 respectively. Firstly, the quartz or synthetic ore pulp was fully mixed for five minutes, with a stirring speed of 1000 rpm. Then, the backwash water pressure and rotation speed were set according to the test parameters' combination in Table 2 to keep the KC in a stable operation condition. Then, the slurry was pumped through a peristaltic pump (BT600, Changzhou PreFluid Technology Co., Ltd., China), which was set at 450 rpm, to the feed hopper of the KC. When the classification process is completed, the concentrate and tailings were collected separately for drying and sample preparation.

For quartz classification tests, the particle size distributions (PSDs) of the tailings and concentrate were measured using a laser particle size analyzer (Bettersize 3000, Bettersize Instruments Ltd., Dandong, China). For synthetic ore classification tests, a magnetic tube (XCGS-Φ50, Tianjin Hualian Mining Instrument Factory, Tianjin, China) was used to separate the quartz and magnetite of the tailings and concentrate before the PSD measurements. The schematic diagram of classification tests is shown in Figure 4.

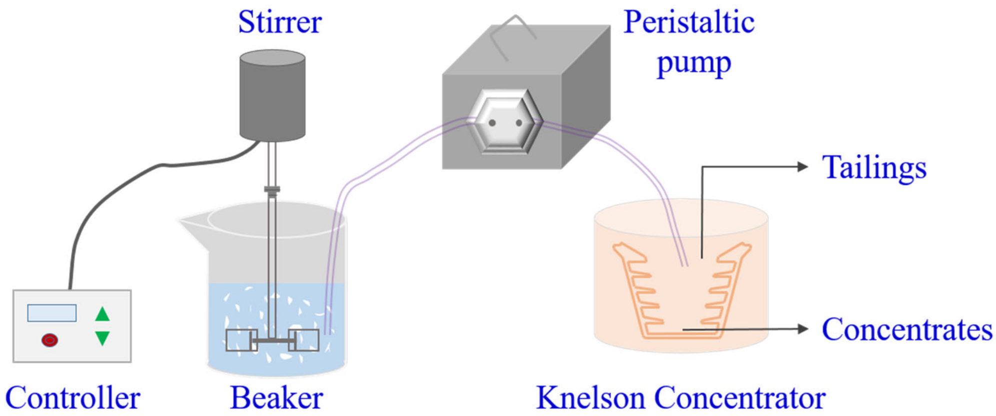

Figure 4. Schematic diagram of classification process.

2.3. Evaluation of Classification Performance

Valid evaluation indicators allow for an accurate assessment of the classification performance of this equipment. The partition curve shows the mass proportion of a specific size class in the concentrate [33]. It is usually plotted on a horizontal log-scale to place emphasis on the fine sizes [34]. The cut size (d_{50}) represents that the particles at that size have a 50% chance of entering the concentrate. The d_{25}, d_{75}, and d_{90} are the same as the d_{50} in definition, and they all can be obtained from the partition curve. The sharpness index (SI) and imperfection (I) of these partition curves are quantified by Equations (1) and (2) [33,35]:

$$\mathrm{SI} = \frac{d_{25}}{d_{75}} \tag{1}$$

$$\mathrm{I} = \frac{d_{75} - d_{25}}{2d_{50}} \tag{2}$$

The larger the sharpness index, the higher the classification accuracy and the classification effect. The smaller the imperfection, the higher the classification accuracy and the classification effect.

In a mineral processing plant, the good or bad classification performance is also evaluated by classification efficiency (CE). The CE represents the proportion of the actual mass of fine particles to the fine particles that would be separated ideally, which can be calculated from Equation (3) [14]:

$$CE = \frac{\beta(\alpha - \theta)}{\alpha(\beta - \theta)} \times 100\% \quad (3)$$

where α represents the mass percentage below the cut size in the feed, %; β is the mass percentage below the cut size in the tailings, %; and θ is the mass percentage below the cut size in the concentrate, %.

3. Results

3.1. Effect of Test Parameters on the Yield of Quartz Concentrate

As depicted in Figure 5a, an overall increase in the yield of the quartz concentrate is observed with an increase in rotation speed. It can be exemplified that the yield of the quartz concentrate increases from 0.43% to 86% when the rotation speed increases from 600 rpm to 3600 rpm, while maintaining a solid mass percentage of 16.67% and a backwash water pressure of 100 kPa. The rise in the rotation speed results in an increase in both the centrifugal force and terminal velocity on the particles, thereby facilitating the sedimentation of particles into the rings as a concentrate.

The results obtained from Figure 5b indicate a decrease in the yield of the quartz concentrate as the backwash water increases, considering different combinations of rotation speed and solid mass percentage. Specifically, the yield of the quartz concentrate is reduced from 80% to 56% when the backwash water pressure increases from 50 kPa to 200 kPa, while maintaining a solid mass percentage of 16.67% and a rotation speed of 2400 rpm. A well-established fluidized bed is formed with the aid of the backwash water pressure. The increase in the backwash water pressure promotes the passage of fine quartz particles through the fluidized bed into the tailings, resulting in a gradual decrease in the yield of concentrate.

Additionally, Figure 5c highlights a general decrease in the yield of the quartz concentrate with an increase in the solid mass percentage. While the yield of the quartz concentrate at a solid mass percentage of 16.67% is close to what is observed at a solid mass percentage of 9.09%, a rapid decline occurs when the solid mass percentage reaches 23.08%. For a backwash water pressure of 100 kPa and a rotation speed of 3600 rpm, the yield of concentrate is at solid mass percentages of 9.09%, 16.67%, and 23.08% are 87%, 86%, and 58%, respectively. It is important to note that, as the KC operates as semi-continuous equipment, a higher solid mass percentage of 23.08% leads to an excessive influx of minerals in the bowl per unit time. Consequently, some particles cannot settle effectively in the rings, resulting in a lower yield of quartz concentrate.

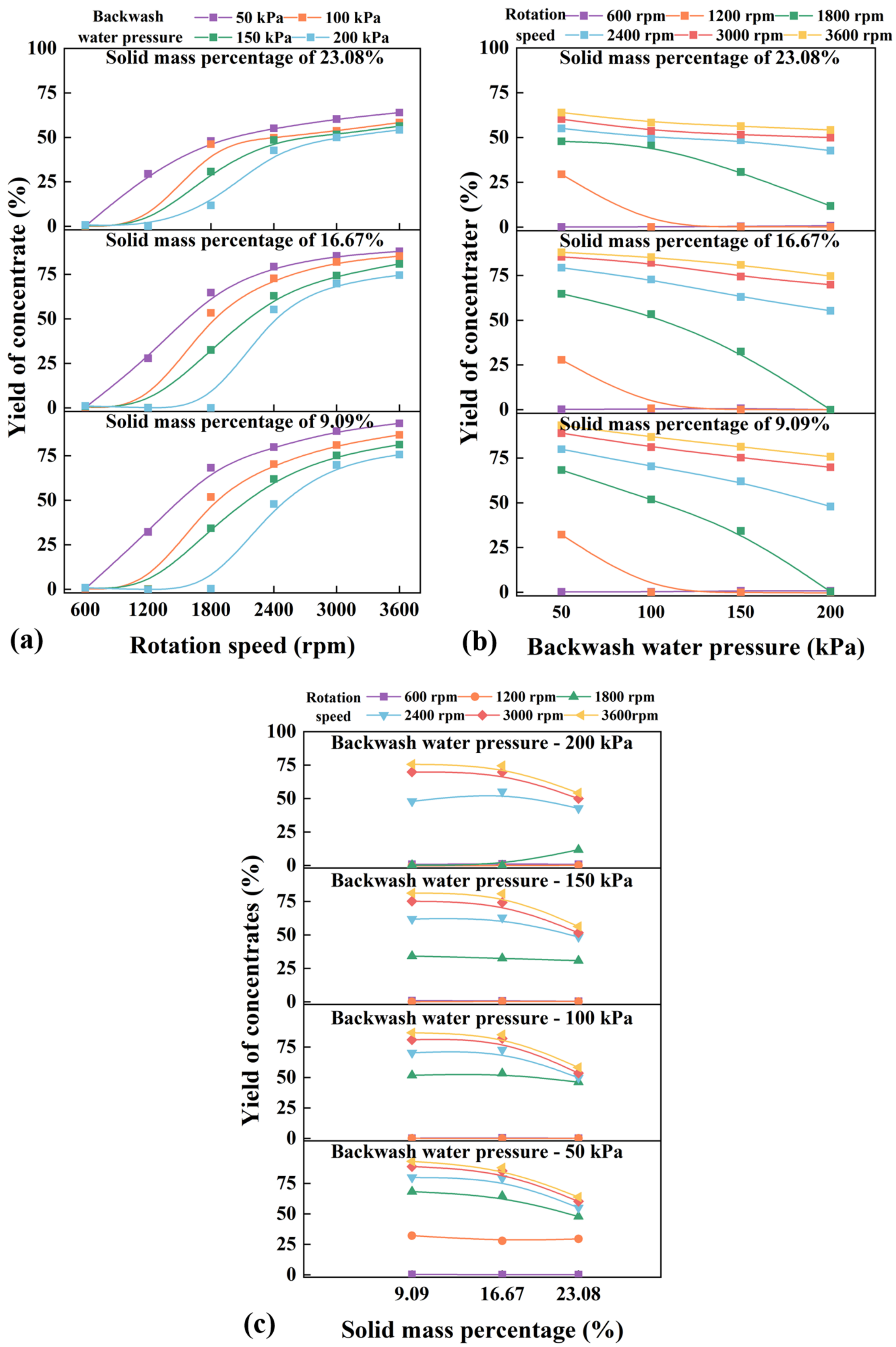

Figure 5. Yield of concentrate as a function of rotation speed (**a**), backwash water pressure (**b**), and solid mass percentage (**c**).

3.2. Effect of Solid Mass Percentage on the Quartz Classification Performance

The solid mass percentage significantly affects the classification performance of quartz. For instance, when considering the test parameters of a rotation speed of 2400 rpm and a backwash water pressure of 100 kPa (as shown in Table 3), the d_{50} value exhibits an upward trend from 93 μm to 225 μm as the solid mass percentage increases from 9.09% to 23.08%, indicating that the cut size gradually increases with the increase in the solid mass percentage, which is because the increase in the pulp concentration will lead to an inadequate classification process. The d_{25} value follows a similar pattern to the d_{50} value. However, the d_{75} and d_{90} initially decrease and then increase with the solid mass percentage. The I reaches a minimum value of 0.40, and both the SI and CE attain a maximum of 0.44 and 81.26%, respectively, when the solid mass percentage is 16.67%, thus indicating that the best classification effect is achieved at a solid mass percentage of 16.67%.

Table 3. Solid mass percentage for the quartz classification performance at a rotation speed of 2400 rpm and a backwash water pressure of 100 kPa.

Solid Mass Percentage/%	d_{25} /μm	d_{50} /μm	d_{75} /μm	d_{90} /μm	I	SI	CE /%
9.09	35	93	218	343	0.98	0.16	73.04
16.67	68	106	158	246	0.40	0.44	81.26
23.08	86	225	333	417	0.55	0.26	75.38

3.3. Effect of Rotation Speed on the Quartz Classification Performance

The rotation speed also plays a significant role in determining the efficiency of quartz classification. Similar to sieving and hydraulic classification, the partition curves exhibit an S-shape at different rotation speeds (Figure 6). When lower backwash water pressure and rotation speed backwash combinations are employed, for instance, 600 rpm/50 kPa, 600 rpm/150 kPa, and 1200 rpm/50 kPa, nearly all the feed quartz particles report to the tailings, thus indicating that the classification effect is poor. These results can be attributed to the insufficient centrifugal force on the quartz particles, which cannot surpass other mechanical forces, such as the drag force and buoyancy force. Consequently, these forces collectively flush the quartz particles into the tailings. With an increase in the rotation speed, the classification phenomena gradually manifest. Table 4 presents the evaluation indexes for the classification performance at a solid mass percentage of 16.67% and a backwash water pressure of 50 kPa.

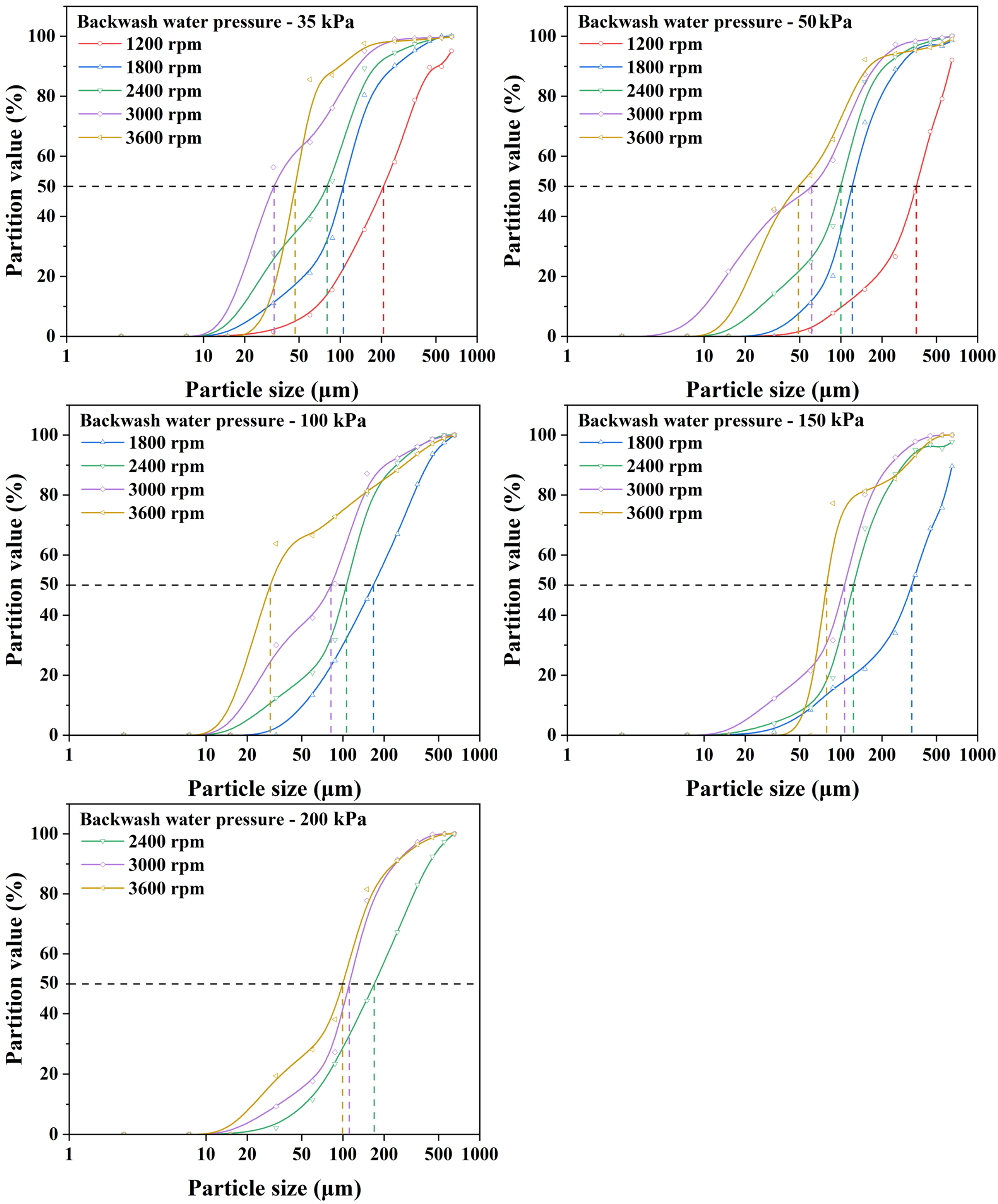

Figure 6. The partition curves of quartz at different rotation speeds and 16.67% solid mass percentage.

Table 4. Rotation speed on the quartz classification performance at a solid mass percentage of 16.67% and a backwash water pressure of 50 kPa.

Rotation Speed /rpm	d_{25} /μm	d_{50} /μm	d_{75} /μm	d_{90} /μm	I	SI	CE /%
1200	220	355	509	633	0.41	0.43	81.30
1800	87	121	176	269	0.37	0.50	89.59
2400	57	100	141	210	0.42	0.41	78.54
3000	17	61	120	180	0.84	0.14	61.45
3600	24	49	105	161	0.84	0.22	76.84

The d_{25}, d_{50}, d_{75}, and d_{90} all decrease with the increase in the rotation speed. At a rotation speed of 1800 rpm, the I reaches its lowest value of 0.37, while both the SI and CE values attain their maximum of 0.50 and 89.59%, respectively, thus highlighting that the classification efficiency is optimal at a rotation speed of 1800 rpm.

3.4. Effect of Backwash Water Pressure on the Quartz Classification Performance

Similar to the solid mass percentage and rotation speed, the backwash water pressure also has a significant impact on the efficiency of quartz classification, and the partition curve also shows an S-shape (Figure 7). When lower rotation speeds are combined with higher backwash water pressures, for instance, 1200 rpm/150 kPa, 1200 rpm/200 kPa, and 1800 rpm/200 kPa, no effective classification occurs, thus leading to the majority of the feed quartz particles entering the tailings. Table 5 illustrates the evaluation indexes of the KC at different backwash water pressures for a solid mass percentage of 16.67% and a rotation speed of 1800 rpm. The backwash water pressure provides the driving force to form a particle fluidized bed, which helps the fine quartz particles to escape from the rings. However, when a larger backwash water pressure is employed, nearly all the feed quartz particles are washed out from the bowl, thus resulting in no effective classification. The d_{25}, d_{50}, d_{75}, and d_{90} increase with the backwash water pressure. The I reached its minimum value of 0.37, while both SI and CE reach their maximum values of 0.50 and 89.59%, respectively, when the backwash water pressure was 50 kPa. These results indicate that the optimal quartz classification efficiency is achieved at a backwash water pressure of 50 kPa.

Table 5. Backwash water pressure effect on the quartz classification performance at a solid mass percentage of 16.67% and a rotation speed of 1800 rpm.

Backwash Water Pressure/kPa	d_{25} /μm	d_{50} /μm	d_{75} /μm	d_{90} /μm	I	SI	CE /%
35	66	105	152	251	0.41	0.44	81.25
50	87	121	176	269	0.37	0.50	89.59
100	86	167	295	413	0.62	0.29	80.49
150	166	330	528	652	0.55	0.31	71.74

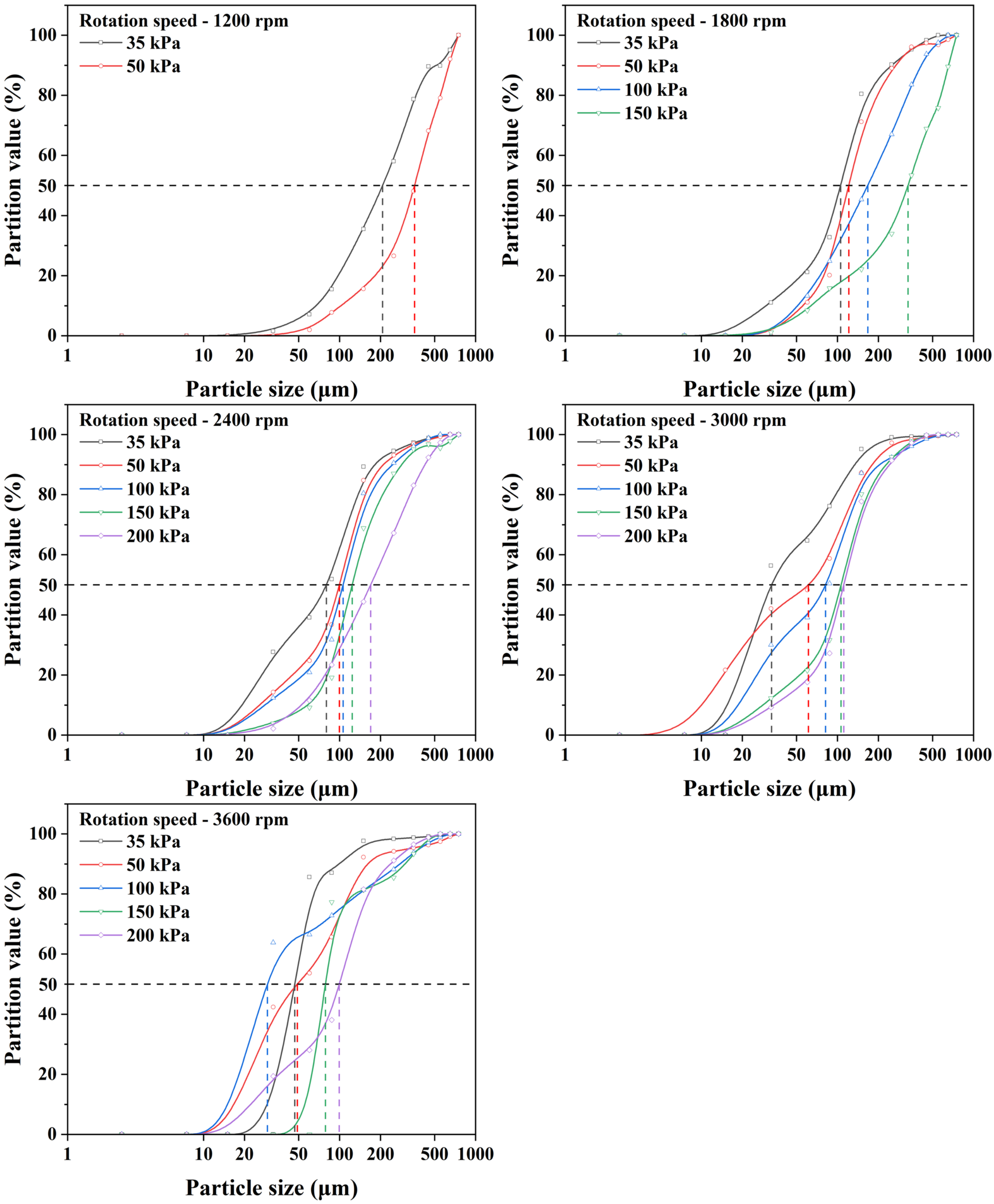

Figure 7. The partition curves of quartz at different backwash water pressures and 16.67% solid mass percentage.

3.5. The Evaluation of Quartz Classification Performance

The CEs of 47 tests are plotted as a ternary phase diagram, as shown in Figure 8. Three parameters, namely the solid mass percentage, backwash water pressure, and rotation speed, form a triangle and are connected counterclockwise, and the values of them are successively distributed on the three sides, from small to large. Inside the triangle, three straight lines parallel to the sides of the triangle are made, and the intersection point and the corresponding point on the *z*-axis are the test variables and the corresponding CE. The values of the CE correspond to the right legend. The *z*-axis represents the CE, and the values of the CE correspond to the right legend. It can be seen from the Figure 8 that the CE values of all tests are greater than 50%. Particularly high CE values exceeding 70% are observed at a low solid mass percentage and backwash water pressure, as indicated by Figure 8. Specifically, the CE and cut size are 76.84% and 49 μm when the solid mass percentage is 16.67%, the backwash water pressure is 50 kPa, and the rotation speed is 3600 rpm.

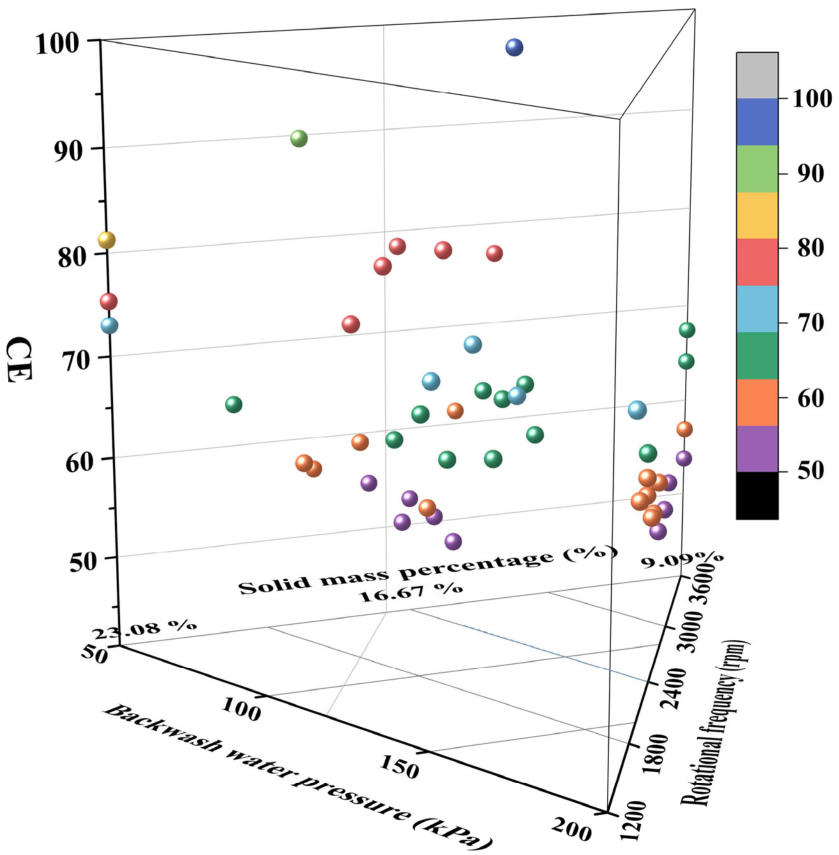

Figure 8. The ternary phase diagram of CE at different test parameter combinations.

A study conducted by Hou et al. [36] investigated the classification performance of quartz particles in different hydrocyclones, and the cut size ranged from 62.21 μm to 120.68 μm. Rasyid et al. [37] also studied the classification performance of semi-inverted hydrocyclones with quartz as the feed. It was observed that the cut sizes were 57 ± 33 μm and 94 ± 27 μm at a position and pressure of 0° and 100 kPa and of 135° and 120 kPa, respectively. The comparison results are shown in Table 6. Although the working principle of the KC and hydrocyclone and the test variables that have an impact on the classification effect are different, the comparison can only be made from some evaluation indicators of the classification effect. Therefore, the d_{50}, a compromise index, was selected to evaluate the classification effect of the KC and hydrocyclone. Nevertheless, these findings indicate that the classification effect of the KC is comparable to that of the hydrocyclones from the research by Hou et al. and Rasyid et al. The noteworthy classification performance of the KC deserves attention and consideration.

Table 6. The classification effects comparison of the KC and hydrocyclones.

Mineral Type	Device	Size Composition (Size Range, Yield)	Test Parameters	Cut Size d_{50}	Reference
Quartz	KC	−0.5 mm, 96.71%	Solid mass percentage, 16.67% Rotation speed, 1200 rpm Backwash water pressure, 50 kPa	49 µm	This study
Quartz	Hydrocyclone	+0.15 mm, 6.52%−0.15 mm, 93.48%	CC type CB type CCC type MS type C type	62 µm 95 µm 75 µm 76 µm 120 µm	Hou et al. [36]
Quartz	Hydrocyclone	−0.096 mm, 80%	Position/° and pressure/kPa 0 and 100135 and 120	57 ± 33 µm 94 ± 27 µm	Rasyid et al. [37]

3.6. The Classification Performance of Synthetic Ore

As can be seen from Figure 9, the yield of quartz concentrate in single quartz and synthetic ore tests increases with the rotation speed at the same backwash water pressure. The yield of single quartz is larger than that of quartz in synthetic ore, and the differences between them gradually increase with the increase in the rotation speed. These findings suggest that the magnetite in synthetic ore impacted the quartz classification process. The yield of magnetite in synthetic ore increases with the increase in the rotation speed and decreases with the increase in the backwash water pressure, as shown in Figure 10.

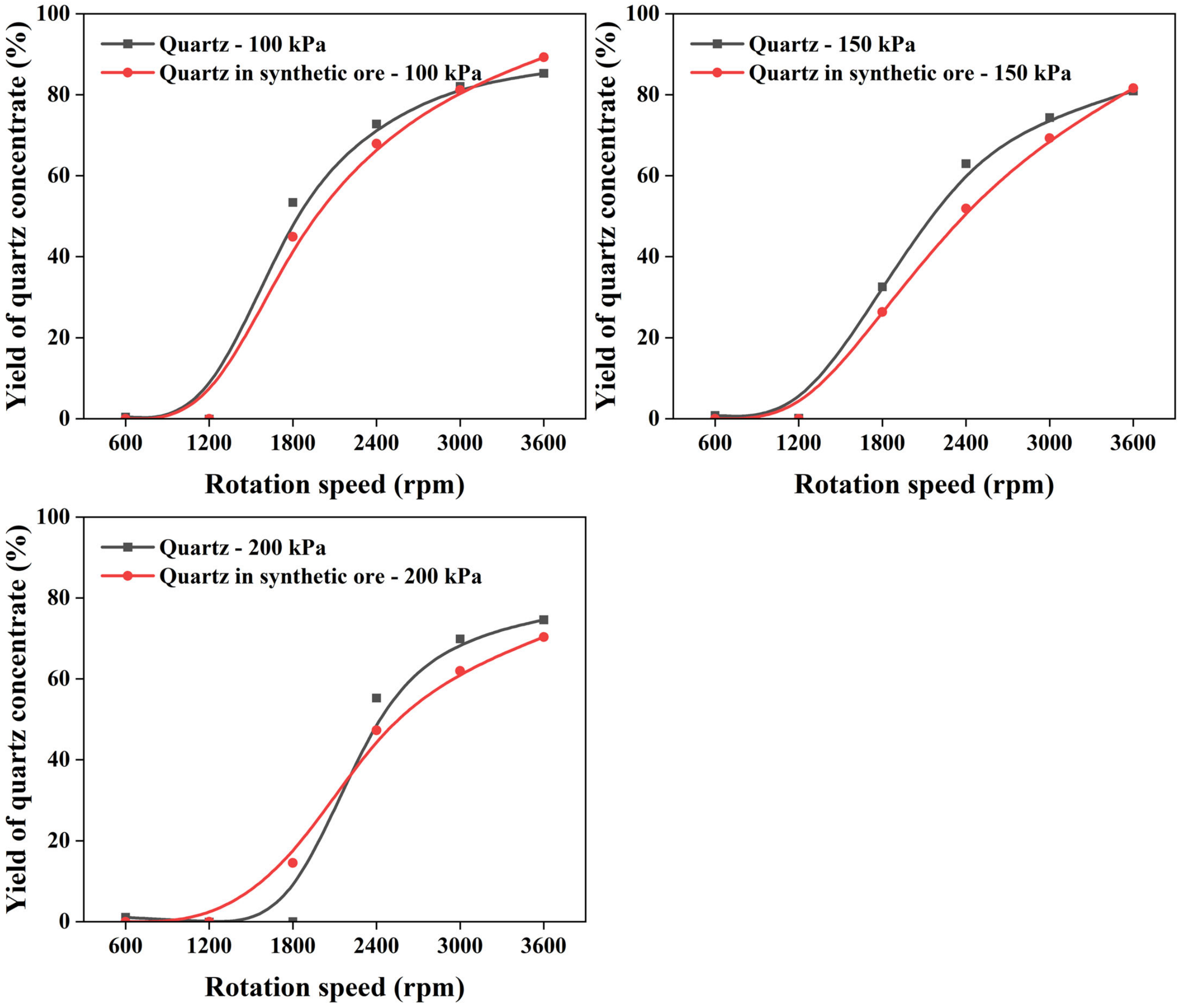

Figure 9. The yield in the quartz concentrate with single quartz and synthetic ore tests.

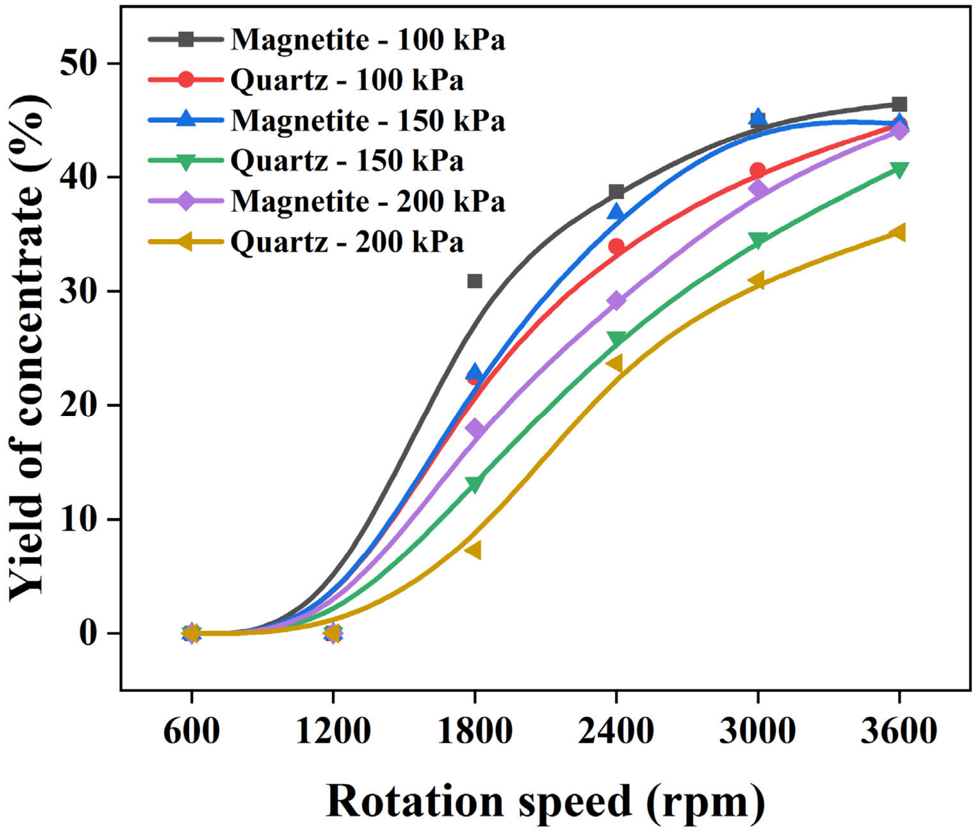

Figure 10. The yield of magnetite concentrate at different backwash water pressures.

The partition curves of quartz and magnetite in the synthetic ore are shown in Figures 11 and 12. A comparison of the partition curves reveals that the quartz partition curves in the synthetic ore do not exhibit an S-shape, while the magnetite partition curves demonstrate a typical S-shape, indicating that the presence of magnetite not only affects the yield of quartz but also influences the classification performance. Table 7 further illustrates that, compared to single quartz, almost all the d_{25}, d_{50}, d_{75}, and d_{90} values of quartz in synthetic ore increase significantly, while the CE decreases substantially. Since magnetite has a higher density and smaller particle size, the slurry concentration of synthetic ore becomes smaller, and, as a result, only coarser quartz particles can settle and enter the concentrate by countering the backwash water, which leads to an increase in the cut size [38].

Table 7. The quartz classification performance with single quartz and synthetic ore tests.

Backwash Water Pressure/kPa	Rotation Speed /rpm	Mineral	d_{25} /µm	d_{50} /µm	d_{75} /µm	d_{90} /µm	I	SI	CE /%
100	2400	Quartz	67	106	152	246	0.40	0.44	80.50
		Quartz in the synthetic ore	32	54	370	582	3.11	0.09	60.44
150		Quartz	89	123	184	286	0.38	0.48	73.72
		Quartz in the synthetic ore	58	203	481	597	1.04	0.41	57.48
200		Quartz	90	169	295	424	0.61	0.31	64.34
		Quartz in the synthetic ore	102	264	461	540	0.68	0.30	62.50

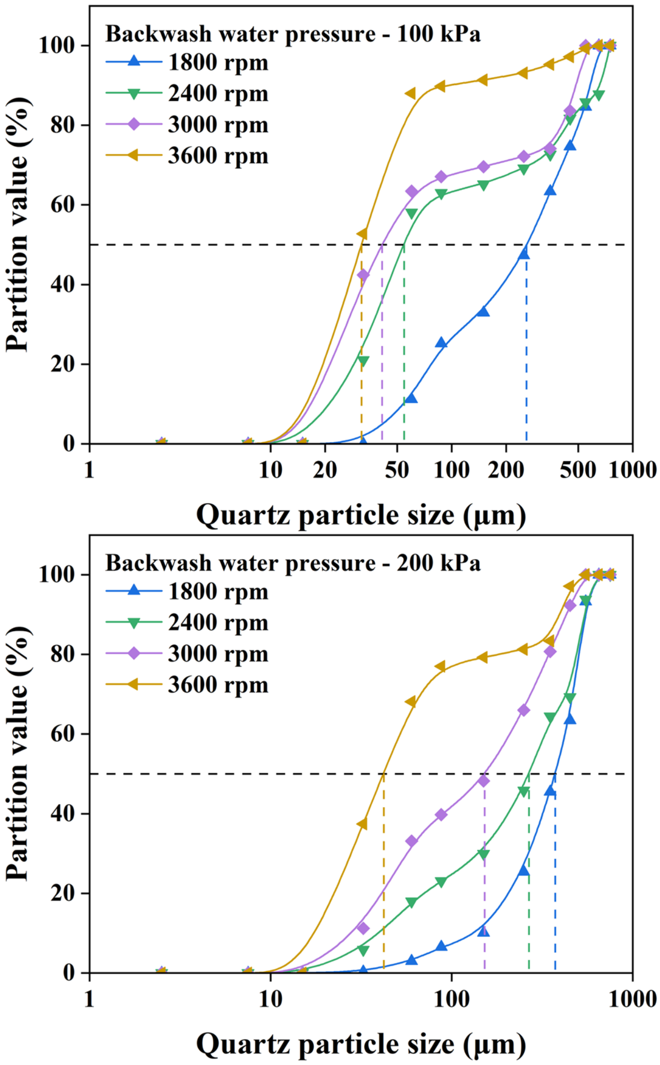

Figure 11. The quartz partition curves in the synthetic ore classification tests at 16.67% solid mass percentage of feed.

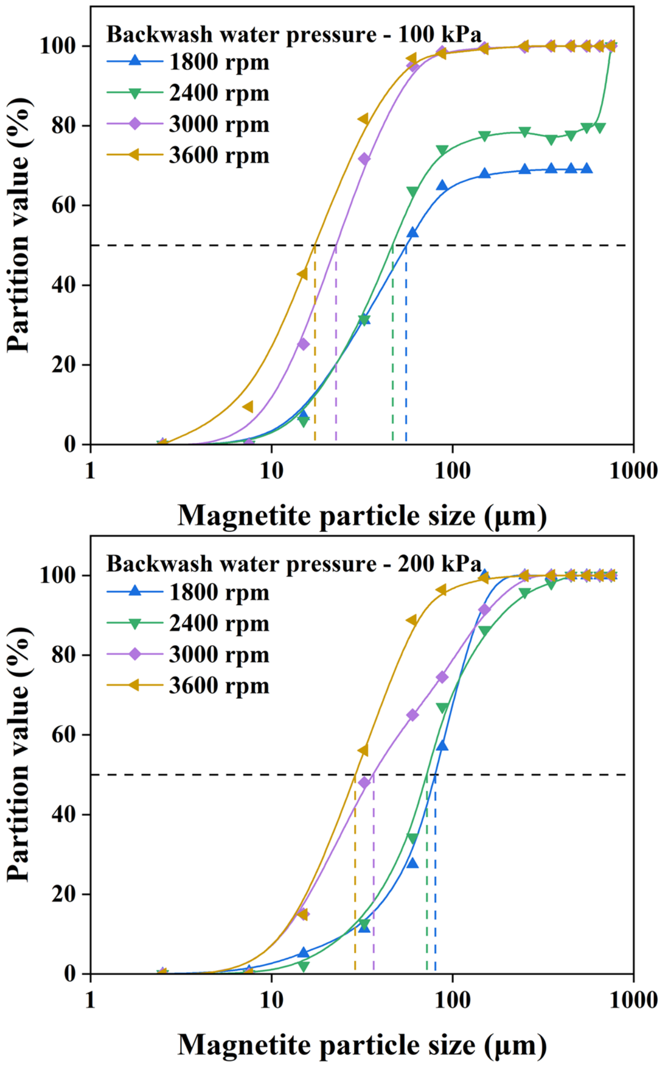

Figure 12. The magnetite partition curves in the synthetic ore classification tests at 16.67% solid mass percentage of feed.

The presented classification size tends to decrease and increase as the rotation speed and backwash water pressure increases, respectively, and the CE ranges from 46.64% to 87.46%, as shown in Table 8. As the density of magnetite is greater than that of quartz and the size of magnetite is smaller than quartz, the d_{25}, d_{50}, d_{75}, and d_{90} of magnetite are smaller than that of quartz. For example, at a backwash water pressure of 150 kPa and a rotation speed of 1800 rpm, the cut sizes of quartz and magnetite are 330 μm and 92 μm, respectively, and the CEs of quartz and magnetite are 71.68% and 87.46%, respectively. The magnetite exhibits a better classification efficiency than the quartz with the same combination of test parameters.

Table 8. The magnetite classification performance at different test parameters.

Backwash Water Pressure /kPa	Rotation Speed /rpm	d_{25} /μm	d_{50} /μm	d_{75} /μm	d_{90} /μm	I	SI	CE /%
100	1800	27	55	106	261	0.72	0.25	46.64
	2400	26	46	37	54	0.12	0.71	61.61
	3000	14	23	-	-	-	-	64.36
	3600	10	17	30	46	0.57	0.34	62.16

Table 8. *Cont.*

Backwash Water Pressure /kPa	Rotation Speed /rpm	d_{25} /μm	d_{50} /μm	d_{75} /μm	d_{90} /μm	I	SI	CE /%
150	1800	62	92	148	245	0.47	0.42	77.04
	2400	27	45	68	100	0.45	0.40	70.35
	3000	15	24	39	58	0.50	0.39	64.42
	3600	15	24	39	57	0.50	0.38	63.53
200	1800	51	80	110	185	0.37	0.47	87.46
	2400	45	72	111	140	0.46	0.40	75.27
	3000	19	36	87	151	0.95	0.21	58.97
	3600	17	29	47	67	0.51	0.37	63.97

4. Conclusions

Three key test parameters, solid mass percentage, backwash water pressure, and rotation speed, which are significantly affecting the classification performances of quartz and synthetic ore were investigated in this study. The yield of the quartz concentrate decreases as the solid mass percentage and backwash water pressure increase, while it increases with the rotation speed. The classification size increases with the solid mass percentage and backwash water pressure, while it decreases with the increase in the rotation speed. Furthermore, the classification efficiency first increases, then decreases, and then reaches the maximum value of 81.26% when the solid mass percentage is 16.67%. An optimum classification performance is reached with the classification efficiency of 89.59%, imperfection of 0.37, and sharpness index of 0.50 at a rotation speed of 1800 rpm and a backwash water pressure of 100 kPa. The cut size of the KC is close to that of some hydrocyclones reported in the literature. Classification tests of synthetic ore composed of magnetite and quartz were conducted to investigate the classification properties of actual minerals. The magnetite increases the settling velocities of the synthetic ore, which leads to a larger classification size of quartz than single quartz tests. The magnetite has a finer classification size and better classification efficiency than quartz. This investigation of particle classification performances in the Knelson concentrator is beneficial for clarifying the migration rule of fine-grained minerals in the enhanced gravity field.

Author Contributions: Conceptualization, methodology, software, L.Z. and L.Y.; validation, L.Z. and D.F.; investigation, resources, data curation, Y.Z., H.H., Z.Z., J.L., C.B. and X.Z.; writing-original draft preparation, L.Y. and L.Z.; writing-review and editing, L.Z., L.Y. and D.F.; visualization, X.Z., J.L., Z.Z. and C.B.; supervision, Y.Z., X.Z. and H.H. All authors have read and agreed to the published version of the manuscript.

Funding: This research was funded by the National Nature Science Foundation of China (52004228), Natural Science Foundation of Shandong Province (ZR2021QE016), Dazhou Scientific Research Project (21ZDYF0006), and Open project of Xinjiang Engineering Technology Research Center of Biological Solid Waste Recycling (KSUGCZX202204).

Data Availability Statement: The data presented in this study may be obtained on request from the corresponding author.

Conflicts of Interest: The authors declare no conflict of interest.

References

1. Hennig, M.; Teipel, U. Grade efficiency for sieve classification processes. *Can. J. Chem. Eng.* **2018**, *96*, 259–264. [CrossRef]
2. Patra, G.; Velpuri, B.; Chakraborty, S.; Meikap, B.C. Performance evaluation of a hydrocyclone with a spiral rib for separation of particles. *Adv. Powder Technol.* **2017**, *28*, 3222–3232. [CrossRef]
3. Nunna, V.; Hapugoda, S.; Pownceby, M.I.; Sparrow, G.J. Application of a Floatex density separator for iron recovery from Pilbara iron ore plant rejects. *Min. Proc. Ext. Met. Rev.* **2022**, 1–8. [CrossRef]
4. Ozcan, O. Performance comparison of a hydrocyclone and crossflow separator-a plant study. *Sep. Sci. Technol.* **2020**, *55*, 799–810. [CrossRef]

5. Zhekalov, N.N.; Bratchikov, V.G.; Ostrovskii, O.P.; Kalachnikova, T.A. Commercial use of hydraulic cyclones and spiral classifiers in systems for dewatering metallurgical sludges. *Metallurgist* **1987**, *31*, 236–237. [CrossRef]
6. Mendoza Quiñonez, J.A.; Pinto, L.R.; Olenka Gómez, J. Rake classifier path as a function of the individual adjustment of its five calibration parameters. *Univ. Cienc. Y Tecnol.* **2016**, *20*, 148–165.
7. Ye, J.; Xu, Y.; Song, X.; Yu, J. Novel conical section design for ultra-fine particles classification by a hydrocyclone. *Chem. Eng. Res. Des.* **2019**, *144*, 135–149. [CrossRef]
8. Hu, Z.; Wang, B.; Bai, Z.; Lu, Z.; Hu, X.; Zhao, S.; Luo, H. Centrifugal classification of pseudo-boehmite by mini-hydrocyclone in continuous-carbonation preparation process. *Chem. Eng. Res. Des.* **2020**, *154*, 203–211. [CrossRef]
9. Mehmet, E.C.; Irfan, K.; Atakan, A.; Ali, S. An experimental investigation into the particle classification capability of a novel cyclone separator. *Sep. Purif. Technol.* **2019**, *209*, 908–913.
10. Neesse, T.; Dueck, J.; Minkov, L. Separation of finest particles in hydrocyclones. *Miner. Eng.* **2004**, *17*, 689–696. [CrossRef]
11. Endres, E.; Dueck, J.; Neesse, T. Hydrocyclone classification of particles in the micron range. *Miner. Eng.* **2012**, *31*, 42–45. [CrossRef]
12. Konrath, M.; Brenner, A.K.; Dillner, E.; Nirschl, H. Centrifugal classification of ultrafine particles: Influence of suspension properties and operating parameters on classification sharpness. *Sep. Purif. Technol.* **2015**, *156*, 61–70. [CrossRef]
13. Vakamalla, T.R.; Koruprolu, K.B.R.; Arugonda, R.; Narasimha, M. Development of novel hydrocyclone designs for improved fines classification using multiphase CFD model. *Sep. Purif. Technol.* **2017**, *175*, 481–497. [CrossRef]
14. Wills, B.A.; Finch, J.A. *Wills' Mineral Processing Technology: An Introduction to the Practical Aspects of Ore Treatment and Mineral Recovery*, 8th ed.; Butterworth-Heinemann: Amsterdam, Netherlands, 2015; pp. 199–220.
15. Nayak, A.; Jena, M.S.; Mandre, N.R. Application of Enhanced Gravity Separators for Fine Particle Processing: An Overview. *J. Sustain. Metall.* **2021**, *7*, 315–339. [CrossRef]
16. Zhang, L.; Yang, F.; Tao, Y. Removal of unburned carbon from fly ash using enhanced gravity separation and the comparison with froth flotation. *Fuel* **2020**, *259*, 116282. [CrossRef]
17. Zhu, X.; Tao, Y.; Sun, Q. Separation of flocculated ultrafine coal by enhanced gravity separator. *Particul. Sci. Technol.* **2017**, *35*, 393–399. [CrossRef]
18. Chen, Q.; Yang, H.; Tong, L.; Niu, H.; Chen, G. Research and application of a knelson concentrator: A review. *Miner. Eng.* **2020**, *152*, 106339. [CrossRef]
19. Marion, C.; Langlois, R.; Kokkilic, O.; Zhou, M.; Williams, H.; Awais, M.; Rowson, N.A.; Waters, K.E. A design of experiments investigation into the processing of fine low specific gravity minerals using a laboratory Knelson Concentrator. *Miner. Eng.* **2019**, *135*, 139–155. [CrossRef]
20. Oediyani, S.; Triana, T.; Ifzan, I.; Mamby, H.E. Centrifugal Concentration of Mandailing Natal North Sumatera Gold Ores Using Knelson Concentrator. *World Chem. Eng. J.* **2021**, *5*, 44–49. [CrossRef]
21. Katwika, C.N.; Kime, M.B.; Kalenga, P.N.M.; Mbuya, B.I.; Mwilen, T.R. Application of Knelson concentrator for beneficiation of copper-cobalt ore tailings. *Min. Proc. Ext. Met. Rev.* **2019**, *40*, 35–45. [CrossRef]
22. Angadi, S.I.; Eswaraiah, C.; Jeon, H.S.; Mishra, B.K.; Miller, J.D. Selection of gravity separators for the beneficiation of the Uljin tin ore. *Min. Proc. Ext. Met. Rev.* **2017**, *38*, 54–61. [CrossRef]
23. Dominy, S.C. Effects of sample mass on gravity recoverable gold test results in low-grade ores. *Appl. Earth Sci.* **2014**, *123*, 234–242. [CrossRef]
24. Gul, A.; Kangal, O.; Ayhan, A.; Guven, S.; Onal, G. Beneficiation of the gold bearing ore by gravity and flotation. *Int. J. Min. Met. Mater.* **2012**, *19*, 106–110. [CrossRef]
25. Ghaffari, A.; Farzanegan, A. An investigation on laboratory Knelson Concentrator separation performance: Part 1: Retained mass modelling. *Miner. Eng.* **2017**, *112*, 57–67. [CrossRef]
26. Ghaffari, A.; Farzanegan, A. An investigation on laboratory Knelson Concentrator separation performance: Part 2: Two-component feed separation modelling. *Miner. Eng.* **2017**, *112*, 114–124. [CrossRef]
27. Özgen, S.; Arsoy, Z.; Ersoy, B.; Çiftçi, H. Coal recovery from coal washing plant tailings with Knelson concentrator. *Int. J. Coal Prep. Util.* **2022**, *42*, 820–830. [CrossRef]
28. Basnayaka, L.; Albijanic, B.; Subasinghe, N. Performance evaluation of processing clay-containing ore in Knelson concentrator. *Miner. Eng.* **2020**, *152*, 106372. [CrossRef]
29. Burat, F.; Baştürkcü, H.; Özer, M. Gold and silver recovery from jewelry waste with combination of physical and physicochemical methods. *Waste Manag.* **2019**, *89*, 10–20. [CrossRef]
30. Xiao, Z.; Laplante, A.R.; Finch, J.A. Quantifying the content of gravity recoverable platinum group minerals in ore samples. *Miner. Eng.* **2009**, *22*, 304–310. [CrossRef]
31. Ghaffari, A.; Farzanegan, A. An investigation on laboratory Knelson Concentrator separation performance: Part 3: Multi-component feed separation modelling. *Miner. Eng.* **2018**, *122*, 185–194. [CrossRef]
32. Chen, Q.; Yang, H.; Tong, L.; Lin, Y.; Ali, A. Ring-by-ring analysis and models of retained mass of quartz in a laboratory Knelson Concentrator. *Miner. Eng.* **2020**, *149*, 106236. [CrossRef]
33. Doroodchi, E.; Zhou, J.; Fletcher, D.F.; Galvin, K.P. Particle size classification in a fluidized bed containing parallel inclined plates. *Miner. Eng.* **2006**, *19*, 162–171. [CrossRef]
34. Frachon, M.; Cilliers, J.J. A general model for hydrocyclone partition curves. *Chem. Eng. J.* **1999**, *73*, 53–59. [CrossRef]

35. Nguyentranlam, G.; Galvin, K.P. Particle classification in the reflux classifier. *Miner. Eng.* **2001**, *14*, 1081–1091. [CrossRef]
36. Hou, D.; Zhao, Q.; Cui, B.; Wei, D.; Song, Z.; Feng, Y. Geometrical configuration of hydrocyclone for improving the separation performance. *Adv. Powder Technol.* **2022**, *33*, 103419. [CrossRef]
37. Rasyid, M.A.; Jokovic, V.; Morrison, R. Classification performance of semi-inverted hydrocyclones. *Miner. Eng.* **2019**, *142*, 105889. [CrossRef]
38. Kim, B.H.; Klima, M.S. Development and application of a dynamic model for hindered-settling column separations. *Miner. Eng.* **2004**, *17*, 403–410. [CrossRef]